Comparative study between in-plasma and post-plasma chemical processes occurring at the surface of UHMWPE subjected to medium pressure Ar and N_2 plasma activation

Parinaz Saadat Esbah Tabaei*, Rouba Ghobeira*, Pieter Cools*, Fatemeh Rezaei*, Anton Nikiforov*, Rino Morent*, Nathalie De Geyter*

* Research Unit Plasma Technology (RUPT), Department of Applied Physics, Faculty of Engineering and Architecture, Ghent University, Sint-Pietersnieuwstraat 41, 9000 Ghent, Belgium

Abstract. Surface chemical properties triggered by plasma activation of polymers were extensively investigated. However, clear distinctions between particular mechanisms occurring in-plasma and post-plasma treatment performed at medium pressure are up-to-the-minute missing and are therefore constituting the study aim. Polyethylene films were subjected to N_2 and Ar plasma using a dielectric barrier discharge operating at 5.0 kPa with a minimally oxygen-contaminated chamber. A distinctive combination of optical emission spectroscopy and *in-situ* X-ray photoelectron spectroscopy (XPS) was used to characterize in-plasma species/surface interactions. Post-plasma oxidation was unraveled by exposing plasma-treated samples to ambient air and performing *ex-situ* XPS. *In-situ* XPS showed remarkably high nitrogen (20.6 %) with negligible oxygen incorporation (2.8 %) thus exceptionally enhancing N-selectivity when comparing to the state-of-the-art. More oxygen (5.9 %) was however detected after Ar activation due to high energy metastables dissociating O_2 impurities. Upon exposure to ambient air, post-plasma oxidation occurred producing more oxygen mainly in the form of O-C=O and N-C=O groups on N_2-activated surfaces and C-O groups on Ar-activated surfaces. Above a certain storage time, physical processes of polymeric chain reorientation prevailed over chemical processes. Overall, in- and post-plasma surface interactions were discriminated in this work that constitutes a perfect-picture reference for polymer plasma activation.

Keywords: N_2 plasma, Ar plasma, *in-situ* XPS, OES, post-plasma oxidation, ageing, polyethylene.

Graphical abstract

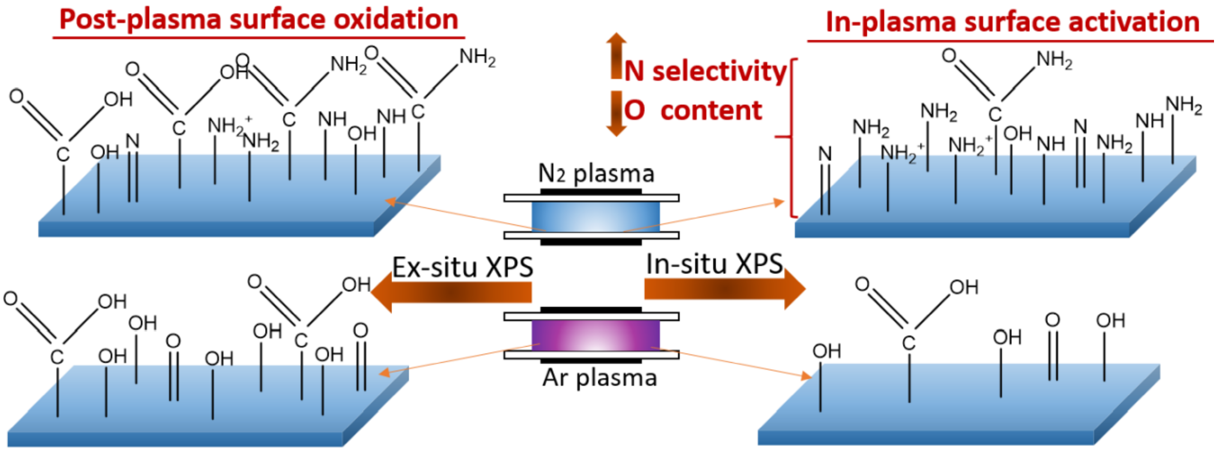

1. Introduction

Within the plasma community, there has been for many years a great interest in better comprehending plasma-polymer surface interactions [1–6]. For this purpose, research groups have been employing a broad range of plasma diagnostic tools and surface analytical techniques such as OES, laser-induced fluorescence (LIF), gas chromatography mass spectrometry (GC-MS), XPS, Fourier-transform infrared spectroscopy (FT-IR), atomic force microscopy (AFM), and time-of-flight secondary ion mass spectrometry (TOF-SIMS), in an attempt to identify and quantify interactions between various plasma discharges and a selection of polymeric substrates and this with a varying amount of success [5,7–16]. To date, there are still two different scientific points of view on how the majority of oxygen is incorporated onto a polymeric surface after treatment with plasma discharges that do not contain oxygen (helium, argon and N_2 discharges being the most popular ones). Some literature reported that during plasma exposure in an oxygen-free atmosphere, the active species in the plasma would primarily produce carbon radicals on the polymer surface through hydrogen abstraction. Following plasma treatment, oxygen containing functionalities would then be incorporated onto the polymer surface due to the reaction of those surface carbon radicals with reactive oxygen molecules (O_2 and H_2O) during exposure to ambient air [10,17–19]. On the other hand, other researchers argued that oxygen functionalities are directly built in on the polymer surface during plasma exposure due to small oxygen impurities being present in the discharge atmosphere, suggesting that post-plasma interactions are of less importance [3,7,20]. For example, Massines et al. observed that by adding only 0.2% of oxygen to an N_2 plasma, the oxygen incorporation on a polypropylene (PP) surface doubled while the nitrogen incorporation significantly decreased [21]. In a first attempt to clarify this, Borcia et al. examined the effect of a nitrogen DBD treatment on the surface of ultrahigh molecular weight polyethylene (UHMWPE) in a controlled atmospheric pressure gaseous environment, unsuccessfully trying to overcome the dominant effect of reactive oxygen plasma species which are typically present in the discharge region due to air contamination. They concluded that the incorporation of oxygen directly occurs on the UHMWPE surface during plasma exposure due to the very high reactivity of unwanted oxygen species in the discharge, even at very low concentrations. Consequently, these researchers also concluded that post-plasma reactions are unlikely to occur [22].

In most available literature on plasma activation of polymers, almost all XPS measurements of plasma treated polymers were carried out after exposing the treated samples to ambient air prior to XPS analysis, hence making it impossible to distinguish between in-plasma and post-plasma oxygen incorporation. At this moment, there are only very few studies in literature dealing with the direct XPS characterization of plasma modified polymer surfaces i.e. without air exposure between the performed plasma treatment and subsequent XPS analysis. In this limited amount of studies, direct XPS analysis was conducted either by making use of a transfer vessel or by connecting the plasma set-up directly to an

XPS machine [10,18,19,23–28]. Additionally, these studies also mainly focused on low pressure plasma activation of polymers. For example, Mutel et al. treated the surface of PP with a low pressure pure N_2 microwave plasma after which the plasma modified PP samples were directly analyzed in an XPS machine without exposure to ambient air (base pressure of the plasma reactor: 2 Pa) [25]. The authors observed a high nitrogen content (≈16 at%) on the PP surfaces upon plasma modification, in combination with an even higher oxygen content (≈ 22 at%). Based on their results, the authors concluded that oxygen incorporation occurs during the nitrogen plasma treatment step due to the presence of oxygen-containing impurities in the nitrogen flow, on the reactor walls and/or in the commercial PP film. In an earlier study, Gerenser employed a low pressure (6.7 Pa) plasma sustained in Ar, O_2, and N_2 atmospheres (base pressure of the plasma reactor: 6.7×10^{-7} Pa) to modify the surface properties of different polymers [19]. Based on the obtained *in-situ* XPS results, the author reported that the performed Ar plasma treatment did not introduce new chemical species onto the polymer surfaces, but can induce degradation and rearrangement of the polymer surfaces. On the other hand, both O_2 and N_2 plasma treatments led to the formation of new chemical species which noticeably altered the chemical reactivity of the polymer surfaces. For example, it was observed that on a polystyrene (PS) surface, oxygen and nitrogen plasma treatment resulted in the incorporation of 18 at% of oxygen and 15 at% of nitrogen respectively. In a later study, Dhayal et al. also performed *in-situ* XPS analysis of Ar plasma modified PS surfaces (base pressure of the plasma reactor: 5×10^{-3} Pa) [24]. These authors observed, in contrast to Gerenser, a significant oxygen incorporation on the PS surface due to the Ar plasma exposure. Based on this short literature overview, it seems that the base pressure of the plasma reactor plays a crucial role in whether oxygen incorporation at the polymer surface directly occurs during plasma exposure. At considerably low plasma reactor base pressures (order 10^{-6}-10^{-7} Pa), oxygen is not incorporated during plasma treatment in Ar or N_2, while at higher base pressures (10^{-3} Pa, 2 Pa), oxygen incorporation directly occurs during Ar/N_2 plasma exposure.

Although considerable progress has been made in unravelling plasma-surface modifications, as can be noticed from the above mentioned literature, some important research aspects have not yet been examined. First of all, literature so far only focused on low pressure plasma treatments, totally neglecting the examination of plasma-surface interactions in case of high pressure plasmas. Additionally, a systematic study examining the impact of post-plasma ambient air exposure on the surface chemical composition of polymers is also lacking. And, last but not least, in the available studies focusing on *in-situ* characterization of plasma treated surfaces, OES diagnostics have been highly underappreciated, although OES is known as a very practical and non-invasive diagnostic technique to determine the nature of excited chemical species inside a discharge. As such, correlating OES diagnostics with direct XPS investigations can aid to fundamentally understand the relative importance of in-plasma and post-plasma reactions on polymeric surfaces. Taking into account these shortcomings in literature, the present work aims to use a combination of OES and direct XPS analysis to examine the relative importance of in-plasma and post-plasma oxygen incorporation on a polymer surface. For this purpose, in contrast to the available literature, a medium pressure plasma sustained in Ar and N_2 will be used, namely a dielectric barrier discharge (DBD) operated at a pressure of 5.0 kPa. Unlike atmospheric pressure plasmas, this medium pressure plasma still allows operating in a controlled gas environment and induces a uniform polymer surface treatment, permitting the study of plasma surface interactions. In this work, UHMWPE is chosen as model polymer. Because of its simple chemical structure ($\text{-(CH}_2\text{-)}_n$) and high chemical inertness (little spontaneous surface oxidation or water adsorption), possible side-effects on the polymer surface will be limited, making it easier to identify and distinguish which surface phenomena are exactly taking place. Besides the direct XPS analysis, a detailed XPS study of the plasma modified UHMWPE samples upon exposure to ambient air will also be conducted in this work. By doing so, we intend to discern the relative importance of in-plasma and post-plasma incorporation of oxygen in case of a medium pressure plasma, to reveal the role of oxygen contamination inside the plasma reactor and to identify which polymer surface changes occur upon storage in ambient air.

2. Materials and methods

2.1. Materials

A roll of UHMWPE with a thickness of 75 µm was purchased from Goodfellow, UK and cut into 1.0 × 1.5 cm^2 pieces without performing any cleaning procedure. N_2 and Ar gases (Alphagaz 1, purity 99.999%) were purchased from Air Liquide, Belgium. Based on the gas specifications provided by Air Liquide, the oxygen and water impurities inside these two gases were assumed to be less than 2 and 3 ppm, respectively.

2.2. Experimental plasma set- up

The schematic of the medium pressure parallel-plate DBD system used in this work is presented in Fig.1 and a detailed description of the set-up can be found in the supporting information (S1.1). As mentioned in the introduction, the main objective of this work was to investigate the polymer surface composition directly after plasma treatment without any air exposure between the plasma modification and the XPS characterization steps. To do so, the DBD plasma chamber was directly connected to an XPS machine and the lower electrode with the polymer sample on top was transferred straight into the XPS introduction chamber using a transfer arm (Fig.1(17)).

In an effort to minimize the level of oxygen contamination inside the plasma reactor, the plasma chamber was continuously kept at high vacuum (pressure of approximately 5 x 10^{-7} kPa) using an Edwards turbo pump (EXT 75DX) directly connected to the plasma chamber. In addition, the polymer samples were introduced into the plasma reactor by first placing them into the introduction chamber of the XPS device. As such, the plasma chamber did not need to be brought to atmospheric pressure to introduce the polymer samples. The low volume intro chamber of the XPS can be easily filled with N_2 to bring it to atmospheric pressure, after which the polymer sample on top of the lower electrode was placed inside the intro chamber. Afterwards, the intro chamber was pumped down to 10^{-3} kPa using the designated rough pump of the XPS machine prior to transferring the sample + electrode into the plasma chamber. After introducing the UHMWPE sample in the plasma reactor, the reactor was pumped down to a pressure of 10^{-3} kPa using a rotary vane pump (Edwards, RV3). For a further reduction of the reactor base pressure, two additional turbo pumps were then switched on: (1) the turbo pump directly connected to the plasma reactor (Edwards, EXT 75DX) and (2) the turbo pump used for evacuating the intro chamber of the XPS device (Pfeiffer vacuum, HiPace 80). By simultaneously using these two turbo pumps, a base plasma reactor pressure of 1 x 10^{-7} kPa could be obtained. Two manometers were used for pressure readings: (1) a Pirani Thyracont VD85 compact vacuum meter (Fig.1(7)) for measuring plasma chamber pressures in the range 10^{2} to 10^{-5} kPa and (2) an Edwards active inverted magnetron gauge (AIM-X-DB40CF) (Fig.1(8)) for accurate measurements of reactor pressures below 10^{-5} kPa. After reaching the desirable base pressure of 1 x 10^{-7} kPa, the plasma reactor was filled with the working gas (Ar or N_2) for 3 minutes using a fixed gas flow rate of 3000 standard cubic centimeters per minute (sccm) making use of a gas mass flow controller (Bronkhorst, El-Flow®) (Fig.1(2)). As a result of this flushing step, the chamber pressure increased to approximately 30 kPa. In a next step, the gas flow rate was reduced to 800 sccm and the plasma reactor was pumped down to 5.0 kPa, after which the plasma was ignited by turning on the high voltage power source. In this work, the gas flow rate, electrode distance, frequency of the applied voltage, the base plasma reactor pressure and the working plasma pressure were kept constant, while the plasma exposure time was varied, as shown in Table 1. For each discharge gas under study, the discharge power was also fixed and the used powers are also presented in Table 1.

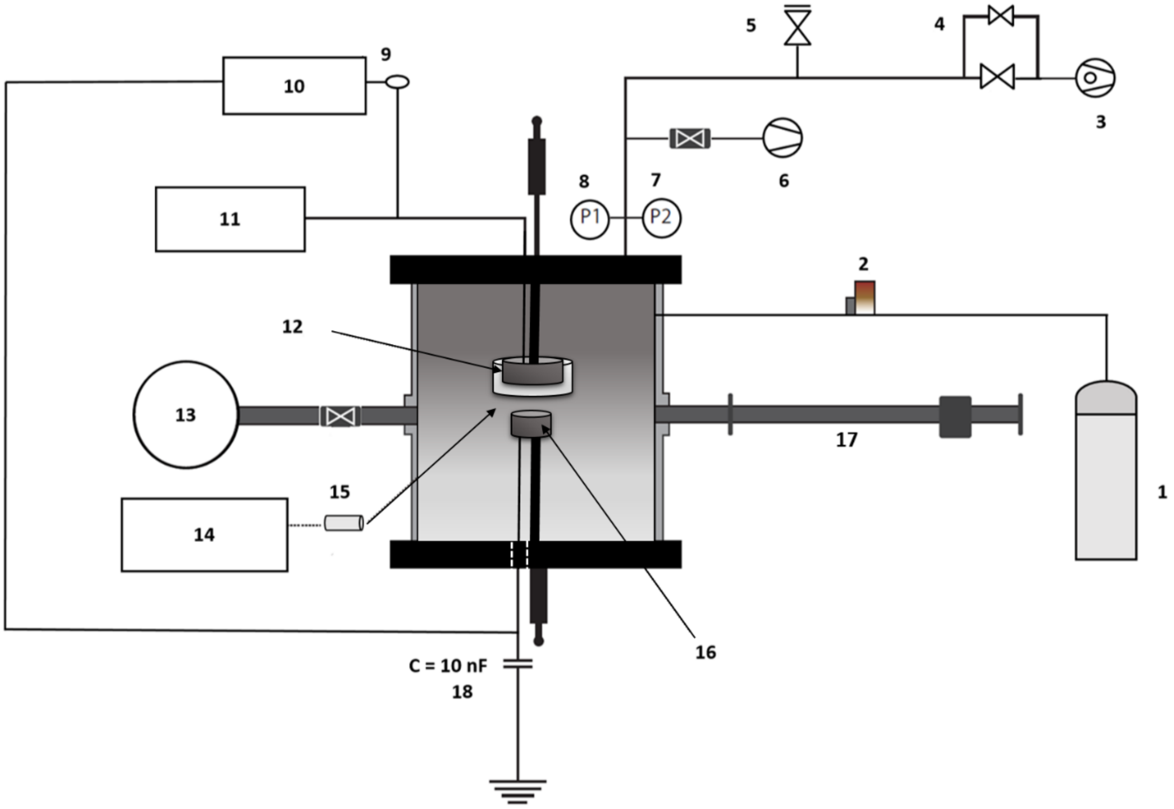

Fig.1 Schematic of the experimental plasma set-up: (1) gas bottle; (2) mass flow controller; (3) rotary vane pump; (4) needle valve; (5) vent; (6) turbomolecular pump; (7) Pirani gauge; (8) active inverted magnetron gauge; (9) high voltage probe; (10) oscilloscope; (11) AC power supply; (12) adjustable powered electrode; (13) XPS machine; (14) optical emission spectrometer; (15) optical fiber; (16) movable substrate holder (bottom electrode); (17) electrode + sample transfer arm; (18) capacitor.

Table 1. Overview of operational parameters for UHMWPE plasma treatments in Ar and N_2

Plasma gas	Discharge power (W)	Treatment time (s)	Energy density at saturated point (mJ/cm^2)*	Gas flow rate (sccm)	Electrode distance (mm)	Frequency (kHz)	Base pressure (kPa)	Working pressure (kPa)
Ar	0.25	0-120	764.3	800	1	20	10^{-7}	5
N_2	0.16	0-90	489.2					

**the saturated point corresponds to the lowest attainable water contact angle (WCA) value, which will be explained in detail in section 3.3*

2.3. Electrical and optical characterization of the discharge

The voltage applied to the top electrode of the reactor was measured using a 1000:1 high voltage probe (Tekronix P6015A), whereas the charge generated on the electrodes was obtained by measuring the voltage over the 10 nF capacitor, connected in series with the discharge reactor to the ground (Fig.1). The obtained charge-voltage waveforms (also known as Lissajous figures) were recorded with a Picoscope 3204A digital oscilloscope, after which the power consumed by the discharge was calculated from these waveforms by using equation 1 as described in [29]:

$$Power = area\ enclosed\ within\ the\ Lissajous\ figure\ \times frequency \qquad (1)$$

$$P = f * \int V(t)C(t)dt$$

where f is the discharge frequency, V(t) the applied high voltage and C(t) the charge on the electrodes as a function of time.

Table 1 also reveals that the applied discharge power is different when using Ar or N_2 as discharge gas. Nevertheless, to be able to objectively compare the surface activation results when using different gas discharges, energy density values (mJ/cm^2) were calculated and the results will be presented in this work as a function of this parameter instead of as a function of treatment time. The energy density was calculated by multiplying the plasma discharge power with the plasma exposure time and by dividing this value by the area of the bottom electrode (Ø: 25 mm) [3].

The optical emission spectra of the N_2 and Ar plasmas were recorded using an optical spectrometer (Ocean Optics, S1000) with a spectral resolution of 0.7 nm in the wavelength range 200 to 900 nm to obtain information on the excited state species present in the discharge. The optical fiber was mounted close to the front window of the reactor and was located 20 cm away from the center of the discharge. Optical emission spectroscopy (OES) analysis of the different discharges was carried out as described by Deng et al. [30]. The obtained OES spectra of the different plasmas were also used to estimate some basic physical characteristics of the discharges under study of which a full description can be found in the supplementary information (section S1.2).

2.4. Surface analysis techniques

2.4.1. Water contact angle measurements

Water contact angle (WCA) measurements were carried out at room temperature in ambient air to pinpoint the saturation region of the performed N_2 and Ar plasma treatments. Additionally, WCA analysis was also performed to determine possibly occurring changes in surface wettability after storing the plasma treated samples in ambient air. Static WCA measurements were performed using a commercial Krüss Easy Drop system immediately after plasma treatment. The deposited water droplets (volume of 2.0 µl) were fitted using Laplace-Young curve fitting and 6 measurements over an extended area of a single sample were collected and averaged.

2.4.2. XPS

XPS measurements were carried out on a PHI Versaprobe II spectrometer employing a monochromatic Al K_α X-ray source (hν = 1486.6 eV) operated at 25 W. All measurements were conducted in a vacuum of at least 10^{-9} kPa and the photoelectrons were detected with a hemispherical analyzer positioned at an angle of 45° with respect to the normal of the sample surface. Survey scans and individual high-resolution spectra (C1s, O1s, N1s) were recorded with a pass energy of 187.85 eV (eV step = 0.8 eV) and 23.50 eV (eV step = 0.1 eV) respectively, using a 100 µm spot size. For all XPS results reported in this paper, 6 measurement points were randomly selected on each sample. Elements present on the surfaces were identified from XPS survey scans and quantified with Multipak (Version 9.6.1) software using an iterated Shirley background and applying the relative sensitivity factors supplied by the manufacturer of the instrument. Multipak software was also used to curve fit the high resolution C1s peaks after calibration of the energy scale using the hydrocarbon component of the C1s spectrum (285.0 eV). The C1s and N1s peaks were deconvoluted using Gaussian–Lorentzian peak shapes (%Gaussian > 80%) and the full-width at half maximum (FWHM) of each line shape was constrained below 1.5 eV. An example of the used C1s and N1s curve fittings can be found in Fig.2.

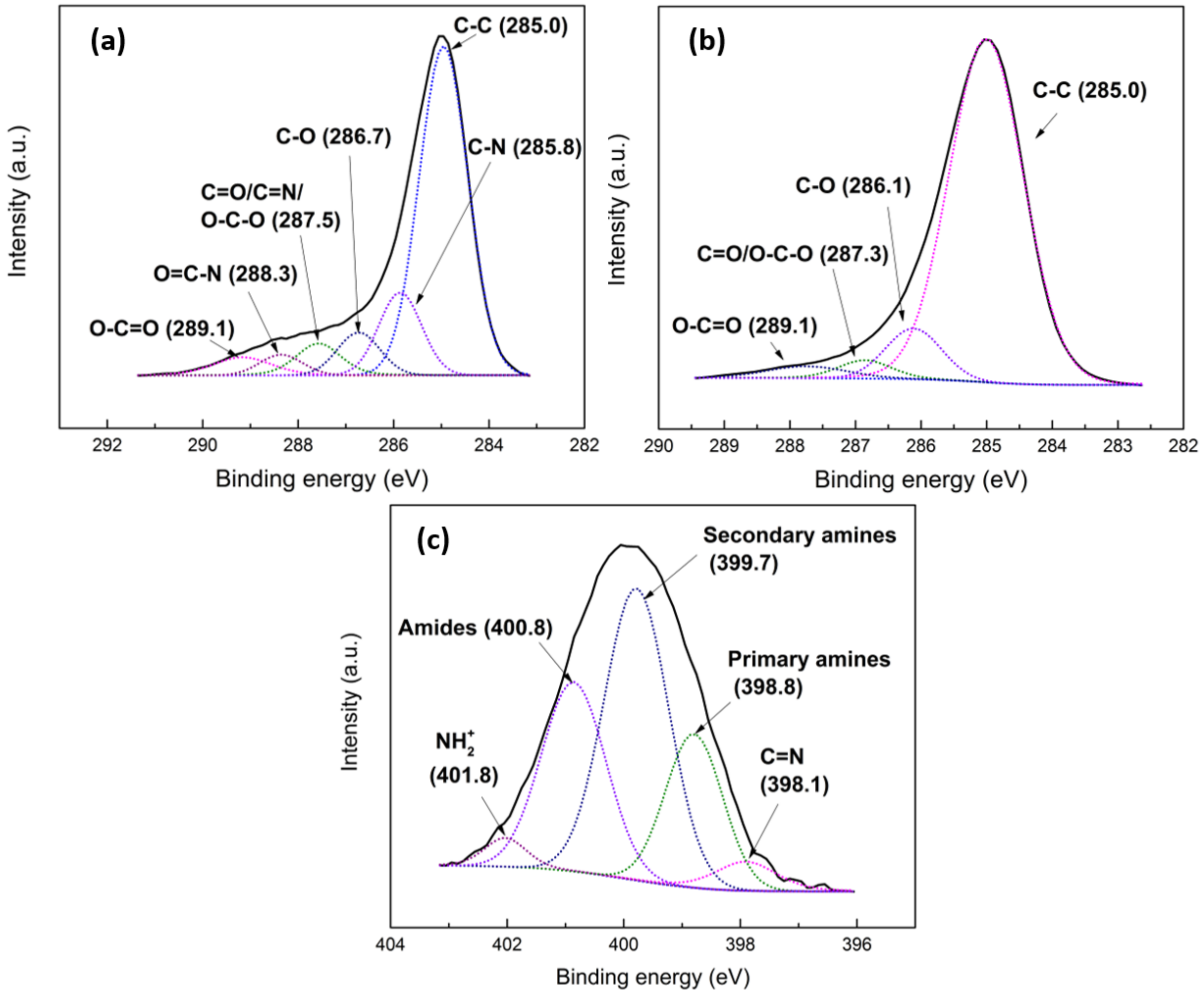

Fig.2 Representation of a typical C1s curve fit in case of N_2 plasma treatment (a), Ar plasma treatment (b) and a typical N1s fitting of an N_2 plasma activated UHMWPE sample after storage in ambient air for 6 hours (c).

3. Results and discussion

3.1. Electrical measurements

The obtained time-averaged Lissajous figures over 15 voltage cycles for N_2 and Ar plasmas are shown in Fig.3. From these Lissajous figures, the discharge power can be calculated and the obtained results have been already given in Table 1: the calculated power for Ar plasma (0.25 W) is higher than that for N_2 plasma (0.16 W). It is well known that the chemically reactive species in the discharge not only depend on the working gas but also on the discharge operational regime [21]. As such, it is also important to reveal information on the operational mode of the DBDs applied in this work. According to literature, the shape of the parallelogram in case of the N_2 plasma depicted in Fig.3 (a) is an indication of a filamentary discharge [34]. In contrast, the Lissajous figure in case of the Ar plasma can be linked to a transition mode of the discharge, operating somewhere between a glow and filamentary mode, often referred to as a pseudo-glow mode [35]. The indication of the operational mode is also confirmed by the visual appearance of the plasma: a homogenous glow discharge uniformly distributed throughout the discharge volume can be seen when using Ar as discharge gas. On the other hand, the discharge in N_2 consists of a set of separate filaments arbitrarily distributed among the electrode surface, confirming the filamentary nature of the N_2 discharge.

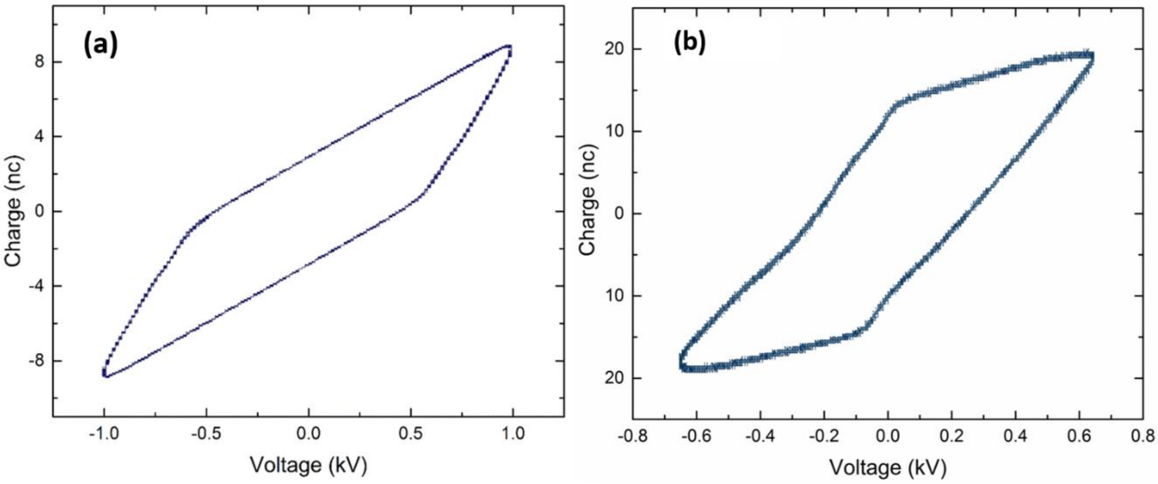

Fig.3 Lissajous figure at 5.0 kPa for (a) N_2 plasma at a discharge power of 0.16 W, (b) Ar plasma at a discharge power of 0.25 W.

3.2. OES study

The normalized OES spectra of the used N_2 and Ar plasma are shown in Fig.4 (a) and (b) respectively and will be discussed in detail in the following paragraphs.

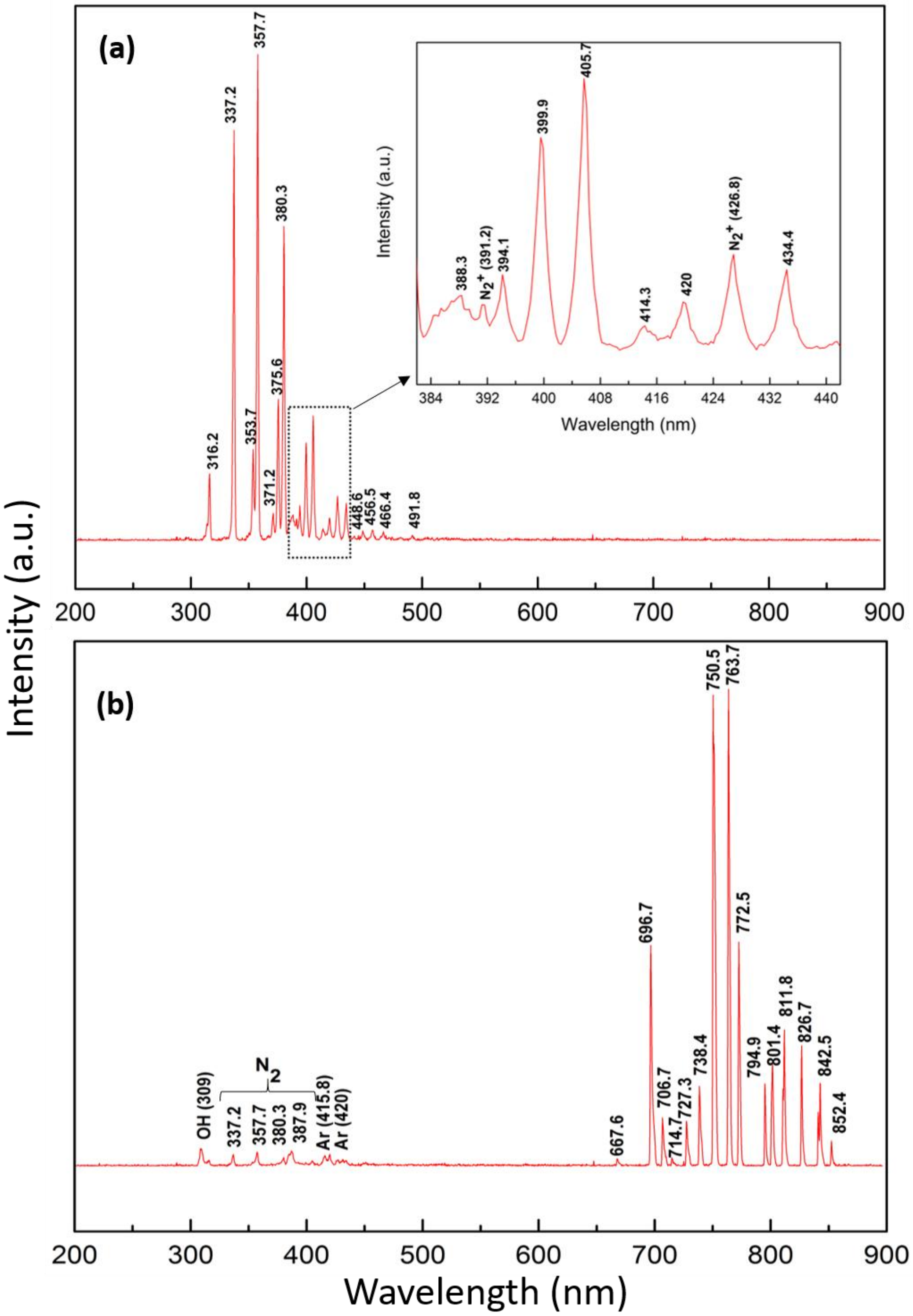

Fig.4 OES spectrum of (a) the applied N_2 plasma and (b) the used Ar plasma.

3.2.1 N_2 plasma spectral analysis

In case of the N_2 plasma, intense OES peaks in the range 316-466 nm can be observed, which can be attributed to the N_2 second positive system, transition $C^3\Pi_u - B^3\,\Pi_g$ [36]. These intense molecular N_2 bands in the OES spectrum thus indicate the presence of electronically and vibrational excited N_2 molecules in the used N_2 plasma. Considering that vibrational excitation of N_2 by electron impact is the most effective at an electron energy between 1.7 and 3.5 eV, it was to be expected that considerable amounts of N_2 vibrational excited states would be present in the used N_2 discharge [37]. Furthermore, as indicated by the research group of Bogaerts et al. [38], the electron impact dissociation of vibrational excited N_2 states is the primary process for the formation of atomic nitrogen through the reaction pathway described below (in its general form) [39]:

$$\mathrm{e^- + \ N_2 \rightarrow N_2(a^1\Pi_g), N_2(B^3\Pi_g), N_2(b^1\Pi_u) + e^- \rightarrow e^- + N + N} \qquad (3)$$

The generation of both vibrational and electronically excited molecular states of N_2 and the subsequent generation of N atoms is of key importance for the effective surface activation of polymers and is the primary source for the incorporation of new N-containing functional groups at polymer surfaces [40]. The emission spectrum, shown in Fig. 4 (a), also indicates the presence of ionized nitrogen molecules (N_2^+) in the discharge, which is confirmed by the appearance of emission lines at wavelengths of 391.2 and 426.8 nm. These spectral lines are known to correspond to the first negative system of the N_2^+ transition $B^2\Sigma_u$-$X^2\Sigma_g$ [30,31]. Additionally, no evidence for the presence of N^+ ions in the N_2 discharge is found in the OES spectrum, leading to the conclusion that N_2^+ is the dominant ionic species in the DBD sustained in N_2 at sub-atmospheric pressure. These N_2^+ species may be possibly generated in the discharge through direct electron impact of ground state N_2 molecules, however, this reaction is less likely to occur as the required electron energy is relatively high (> 15.6 to 18.5 eV) [41]. More likely is the stepwise generation of N_2^+ through electron impact ionization processes with vibrational excited N_2 states [36,42]. Fig.S1 in the supporting information also shows that the formation of excited N_2^+ species is more pronounced when the plasma reactor base pressure is lowered to 10^{-7} kPa. Finally, it is also important to mention that at the working pressure of 5.0 kPa, the plasma source operates in the recombination mode and diffusion loss of N_2^+ could be neglected [31,43]. The major portion of the N_2^+ ions will thus recombine with free electrons through dissociative recombination, resulting in the formation of $N(^4S)$ (atomic state), $N(^2D)$ and $N(^2P)$ (metastables) with a relative abundance of ~1, ~ 0.9 and < 0.1 respectively [44]. This process is considered to be important as the N metastable states ($N(^2D)$ and $N(^2P)$) and nitrogen atoms, generated by dissociative recombination as well as by the reaction given in Eq. 3, are known to play a major role in altering the surface chemistry [40] as will be discussed later in this work.

3.2.2 Ar plasma spectral analysis

The OES spectrum of the DBD sustained in Ar is characterized by intense Ar I lines (4p-4s) found in the wavelength range 696-852 nm [33,45], and less intensive Ar I lines (5p-4s) which appear in the wavelength region between 415 and 420 nm [33,45,46]. As can be seen in the Fig.4 (b) and also in the supporting information (Fig.S1), a small emission line attributed to OH radicals is also visible in the OES spectrum of the Ar discharge at 309 nm. Additionally, also a set of emission lines is present in the wavelength range 337-399 nm which can be attributed to the N_2 second positive system. The appearance of other peaks besides Ar emission lines thus indicates the presence of trace amounts of contamination in the Ar discharge, even when reaching a base reactor pressure of 10^{-7} kPa. Nevertheless, it can also be observed from Fig.S1 that the amount of the contaminants in the Ar discharge can be considerably reduced when the base reactor pressure is decreased to its lowest attainable value (10^{-7} kPa). It is also important to note that not a single trace contaminant, such as for example OH radicals (309 nm), atomic oxygen (777 nm) or atomic hydrogen H_α (656 nm) could be observed in the OES spectrum of the N_2 discharge, not even at high plasma reactor base pressures of 10^{-5} or 10^{-6} kPa (Fig.S1). This can be related to the fact that all above-mentioned impurities (OH, O and H_α) are created by dissociation of trace molecules, namely H_2O and O_2. This dissociation process followed by excitation is however very inefficient in case of an N_2 discharge due to the low electron temperature as the dissociation process typically requires high energy values above 10 eV. Consequently, no trace contaminations derived from H_2O and O_2 could be observed in the OES spectrum of the used N_2 discharge, although they are definitely present in the discharge reactor. On the other hand, in the Ar discharge, highly energetic Ar metastables with energies above 13 eV are present, which can effectively dissociate trace impurities, resulting in the presence of OH radicals in the OES spectrum of Ar (Fig.4 (b) and S1).

Finally, it is also important to mention that OES is a recognized technique capable of detecting excited states which are emitting photons due to radiative decay. In both Ar and N_2 discharges, there are however also considerable amounts of metastables being generated which are considered to be key species in both plasma chemistry and polymer-surface interactions [47]. Unfortunately, measuring and detecting these metastables is not possible with OES as their radiative depopulation to the ground state is forbidden. However, to get more insight in the plasma properties, the electron excitation temperature (T_{exc}) of the discharges under study was also determined from OES spectra. The results of these measurements are provided in the supporting information (section S2.2).

3.3. WCA results as a function of energy density

Fig.5 represents the WCA evolution of the Ar and N_2 plasma treated UHMWPE films as a function of energy density. Within this context, it is worth mentioning that WCA measurements were carried out solely on plasma treated samples which were exposed to ambient air after plasma modification (referred to as “indirect” samples in this work) because it was not possible to determine the treatment efficiency with WCA analysis without any exposure to ambient air. This WCA analysis was performed to select the optimal energy density values (or the optimal plasma exposure time) for both discharges under study as only the samples exposed to these optimal conditions will be subjected to XPS analysis.

Fig.5 reveals that the WCA on the UHMWPE samples progressively decreases with increasing energy density for both N_2 and Ar plasma treatments until a rather constant, so-called saturated WCA value was reached (N_2 = 41.3° ± 3.3 ; Ar = 61.5° ± 3.4), similar to what was observed in earlier work [29,48,49]. Fig.5 also shows that the treatment in N_2 plasma appears to be more effective in reducing the WCA values on the UHMWPE substrates compared to the Ar plasma treatment. Furthermore, the energy density required for reaching the minimal attainable water contact angle was higher for the Ar discharge than in case of the N_2 discharge, as can be seen from the values mentioned in Table 1. According to literature, N_2 plasma treatments typically lead to the simultaneous incorporation of oxygen and nitrogen containing polar groups such as amines, amides, peroxides, alcohols, aldehydes, esters, … onto the surface of a plasma exposed polymer [7,22]. In contrast, in case of an Ar plasma treatment, typically only oxygen containing polar groups are being incorporated, leading to a less profound increase in polymer surface wettability [21,29,50–52]. Additionally, as oxygen species are only present as contamination in the Ar and N_2 discharge and nitrogen species are abundantly present in the N_2 plasma (see OES results), it also appear logic that longer plasma treatment times are needed in case of Ar plasma to reach the highest attainable surface wettability. To obtain a deeper knowledge on the UHMWPE surface chemistry after plasma treatment, XPS measurements have been performed on untreated and plasma treated UHMWPE surfaces exposed to the optimal energy density values, which are indicated in Table 1, as the largest differences in surface chemical composition are to be expected for these samples. The obtained XPS results will be extensively described in the following results section.

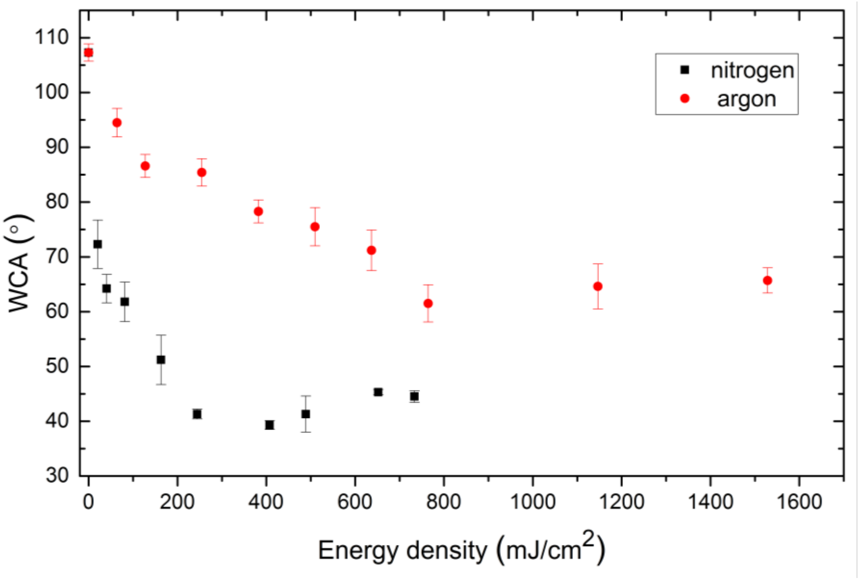

Fig.5 WCA evolution on UHMWPE samples as a function of energy density in case of Ar and N_2 plasma treatment

3.4. XPS results

3.4.1. N_2 plasma treatment

Table 2 represents the atomic composition, determined from XPS survey spectra of the untreated and the N_2 plasma treated UHMWPE sample for 2 particular conditions: (1) without exposure to ambient air between plasma treatment and XPS analysis (so-called direct XPS analysis) and (2) with exposure to ambient air for different durations ranging from 5 minutes to 21 days (so-called indirect XPS analysis). From table 2, it can be seen that the untreated UHMWPE film already contains a small amount of oxygen, which could be mainly attributed to surface contamination. Table 2 also shows that N_2 plasma treatment itself results in a significant nitrogen incorporation on the UHMWPE sample (20.6 ± 0.8 at% for the plasma-treated sample compared to 0 at% for the untreated sample). The abundant incorporation of nitrogen containing functional groups on the surface can be explained by the following mechanism: excited nitrogen molecules in the discharge are able to break C-C and/or C-H bonds on the polymer surface resulting in the formation of polymer radicals. These radicals will in turn rapidly react with atomic and metastable nitrogen states, namely $N(^4S)$, $N(^2p)$,… present in the discharge resulting in the grafting of nitrogen containing functional groups on the polymer surface [21,40].

Table 2 also reveals that during the N_2 plasma treatment, a small amount of oxygen is also incorporated into the UHMWPE samples as the surface oxygen content increases from 1.1 ± 0.1 at% to 2.8 ± 0.4 at% resulting in an O/C ratio of 0.03 after plasma modification. When comparing the observed oxygen incorporation with other studies available in literature, it can be concluded that the N_2 plasma treatment in this work only introduces a very small amount of oxygen to the UHMWPE surface. Indeed, in other studies, authors have reported O/C ratios varying between 0.12 and 0.24 after N_2 plasma treatment of UHMWPE [22,48,49]. The lower oxygen incorporation in this particular work can be mainly attributed to the presence of less oxygen impurities in the used plasma reactor as the reactor base pressure is set to 10^{-7} kPa. In the work of Aziz et al., a much higher reactor base pressure of 0.05 kPa was used [53], while in the paper of Borcia et al. plasma treatment was performed at atmospheric pressure using high nitrogen gas flows to maximally eliminate oxygen contamination [22]. Thanks to the low oxygen contamination in the N_2 discharge used in this work, considerably large amounts of nitrogen could also be incorporated at the UHMWPE substrate resulting into an N/C ratio of 0.26. In contrast, when N_2 plasma treatments were performed in reactors containing high levels of oxygen contamination, much lower N/C ratios have been reported (0.08 to 0.17) [22,49,53]. Oxygen, present even at very low levels, is indeed known to be a very surface reactive species and can thus strongly hamper the incorporation of nitrogen at the polymer surface [7,22]. This work thus clearly reveals the large impact of oxygen traces inside a nitrogen discharge: the more oxygen contamination can be removed from the discharge, the more nitrogen can be incorporated at the polymer surface. Experiments conducted by the authors of this paper (results shown in Table S1 of the supplementary information) have indeed revealed that the oxygen incorporation becomes more pronounced and the nitrogen incorporation less intense when higher plasma reactor base pressures were used.

Table 2 also reveals that by exposing the N_2 plasma treated samples to ambient air for only 5 minutes, the oxygen incorporation at the UHMWPE surface significantly increases to 6.1 ± 0.2 at%. The increase in oxygen content upon ambient air exposure may be attributed to the rapid reaction between oxygen and/or water vapor present in ambient air and radicals and/or nitrogen containing functional group present on the surface of the N_2 plasma modified UHMWPE samples, thereby resulting in post-plasma oxygen functionalization [17]. Indeed, plasma treatment is known to induce breaking of the polymer C-C/C-H bonds thereby resulting in the formation of polymer radicals [3,54]. In the following paragraph focusing on XPS fitting, it will be examined if ambient air interacts with remaining surface radicals and/or nitrogen functional groups at the polymer surface upon storage in air. Table 2 also shows XPS results for longer exposure times to ambient air, however, these results will be discussed in the last part of this study focusing on the ageing behavior of the plasma modified UHMWPE samples. To conclude, it can be stated that thanks to the low plasma reactor base pressure used in this work, direct oxygen incorporation during N_2 plasma treatment is quite low and most of the observed surface oxygen upon exposure to ambient air can thus be attributed to post-plasma reactions. In case higher plasma reactor base pressures are used, oxygen incorporation will however mostly occur during N_2 plasma treatment (see Table S1) and post-plasma oxidation effects will be of less importance.

Table 2. Surface chemical composition of the N_2 plasma modified UHMWPE samples without and with exposure to ambient air during different time periods ranging from 5 min to 21 days

Sample	**C1s (at%)**	**N1s (at%)**	**O1s (at%)**	**O/C**	**(N+O)/C**	**N/C**
Untreated	98.9 ± 0.0	0	1.1 ± 0.1	0.01	0.01	0
Direct	76.6 ± 0.5	20.6 ± 0.8	2.8 ± 0.4	0.03	0.30	0.26
5 min	74.1 ± 0.9	19.8 ± 0.5	6.1 ± 0.2	0.08	0.34	0.26
30min	75.2 ± 1.8	18.6 ± 2.1	6.2 ± 0.3	0.08	0.33	0.24
1 h	75.3 ± 1.6	17.3 ± 2.0	7.4 ± 0.7	0.09	0.33	0.23
3h	73.9 ± 1.9	18.8 ± 2.0	7.3 ± 0.2	0.09	0.35	0.25
4h	74.0 ± 0.7	18.7 ± 0.6	7.3 ± 0.04	0.09	0.35	0.25
5h	74.7 ± 0.6	17.5 ± 0.3	7.8 ± 0.3	0.10	0.33	0.23
6h	74.4 ± 0.5	17.3 ± 0.5	8.3 ± 0.5	0.11	0.34	0.23
24 h	73.8 ± 1.7	17.6 ± 1.2	8.6 ± 1.1	0.11	0.35	0.23

21 days	84.0 ± 1.4	8.1 ± 1.3	7.9 ± 0.6	0.09	0.19	0.09

To reveal more information on the type of functional groups incorporated on the UHMWPE surface upon N_2 plasma treatment, high resolution C1s and N1s peaks have also been fitted according to the procedure described in the materials & methods section. In case of the untreated UHMWPE sample, **C**-C and **C**-O peaks at 285.0 and 286.7 eV (the latter due to surface contamination) were used to obtain a good C1s fit. In contrast, the C1s peaks of the N_2 plasma modified samples were fitted using 6 different peaks, as shown in Fig.2 (a): **C**-C, **C**-N, **C**-O, **C**=O/**C**=N/O-**C**-O, O=**C**-N and O-**C**=O at 285.0, 285.8, 286.7, 287.5, 288.3 and 289.1 eV respectively [36,52,55,56] Based on these C1s XPS fittings, the relative concentration of each carbon-containing surface functional group could be obtained and the results are presented in Table 3. These results clearly reveal that the performed N_2 plasma treatment results in the simultaneous incorporation of different polar functionalities including C-N, C-O, C=O/C=N/O-C-O and O=C-N groups on the UHMWPE surface. After storing the N_2 plasma modified sample in ambient air for 5 min, no significant differences can be seen in the concentration of C-N, C-O, C=O/C=N/O-C-O and O=C-N functional groups. On the other hand, a notable increase in O=C-O groups after a short exposure to ambient air is observable: this increase could be explained by the reaction of remaining free carbon-centered surface radicals ($C^{\bullet}$) after N_2 plasma treatment with ambient oxygen leading to the formation of metastable peroxy radicals and hydroperoxides, which can further decompose to generate a variety of stable functional groups, such as hydroxyl, carbonyl and carboxylic functional groups [57]. In this particular case, mainly carboxylic functional groups seem to appear due to the post-plasma oxidation processes.

Table 3. Relative concentrations (in %) of carbon containing functional groups on UHMWPE samples after N_2 plasma treatment

Bands	Untreated	Direct	5 min	30 min	1 h	3 h	4 h	5h	6 h	24 h	21 days
C-C	95.3 ± 0.5	70.6 ± 0.7	63.8 ± 2.6	68.4 ± 2.5	67.4 ± 1.1	69.5 ± 2.5	66.9 ± 3.7	65.8 ± 0.8	66.1 ± 2.6	67.0 ± 3.3	75.2 ± 1.4
C-N	-	14.7 ± 2.6	15.4 ± 2.3	13.6 ± 2.7	13.5 ± 1.8	14.8 ± 3.3	13.5 ± 4.9	14.9 ± 1.3	15.0 ± 2.6	13.9 ± 1.2	13.5 ± 2.1
C-O	4.6 ± 0.5	6.3 ± 2.2	8.5 ± 0.6	6.2 ± 1.4	7.9 ± 1.6	6.6 ± 1.4	7.6 ± 1.4	6.2 ± 1.0	6.4 ± 1.7	7.0 ± 0.9	7.7 ± 2.2
C=O/C=N/O-C-O	-	5.7 ± 0.7	6.1 ± 0.7	5.8 ± 1.1	4.1 ± 2.0	4.0 ± 1.0	5.4 ± 1.0	6.8 ± 2.3	4.6 ± 0.8	4.9 ± 0.8	2.1 ± 0.3
O=C-N	-	2.6 ± 0.5	3.4 ± 0.8	3.8 ± 0.8	4.3 ± 2.0	3.6 ± 0.6	3.7 ± 0.3	2.5 ± 0.8	5.1 ± 0.8	4.4 ± 1.3	1.2 ± 0.2
O=C-O	-	0.1 ± 0.2	2.8 ± 0.9	2.2 ± 0.7	2.8 ± 0.6	1.5 ± 0.6	2.9 ± 0.5	3.7 ± 0.3	2.6 ± 0.8	2.8 ± 1.2	0.1 ± 0.2

Table 4. Relative concentrations (in %) of nitrogen containing functional groups on UHMWPE samples after N_2 plasma treatment

Bands	Untreated	Direct	5 min	30 min	1 h	3 h	4 h	5 h	6 h	24 h	21 days
C=N	-	7.7±2.1	5.7±2.1	6.9±2.0	5.9±1.5	4.8±3.2	4.3±1.7	6.0±1.4	5.3±1.6	5.9±2.0	4.7±1.7

Primary amines	-	29.9±3.3	25.4±3.9	24.4±3.7	22.2±2.8	24.6±6.4	22.2±2.3	20.8±4.6	22.1±2.7	19.9 ±2.5	29.5±4.9
Secondary amines	-	39.2±2.3	40.1±1.8	41.6±2.4	42.9±1.8	42.7±5.0	43.5±3.1	41.4±3.0	39.4±2.5	42.9±3.5	37.3±3.1
Amides	-	17.5±0.8	21.9±1.3	21.3±2.2	25.2±1.4	24.6±3.1	25.7±0.9	26.9±2.7	28.0±3.4	25.9±1.4	23.9±1.0
NH_2^+	-	5.7±0.9	6.9±2.7	5.8±1.6	3.8±1.3	3.3±1.7	4.3±0.9	4.9±2.1	5.2±1.8	5.1±1.8	4.4±2.7

Besides fitting the high resolution C1s peaks of the N_2 plasma modified samples, also the high resolution N1s peaks have been curve fitted in an effort to reveal more information on the type and concentration of the nitrogen containing functional groups. The N1s peaks have been fitted making use of 5 different peaks, as depicted in Fig.2 (c): C=**N**, **N**H_2 (primary amines), **N**H (secondary amines), **N**-C=O (amides) and **N**H_2^+ at 398.1, 398.8, 399.7, 400.8 and 401.8 eV respectively [58–60]. From these fittings, the relative concentrations of the nitrogen functional groups have been determined and the results are presented in Table 4. According to this table, the actual N_2 plasma treatment mainly results in the incorporation of primary and secondary amines and to a lesser extent amides, which is consistent with the results from the C1s curve fitting. Table 4 also reveals that upon 5 min exposure to ambient air, a significant increase in the amount of amides occurs, which was not well observed in the C1s curve fitting due to the low contribution of the amide groups to the total C1s peak. Post-plasma oxidation processes therefore do not only result into the incorporation of O-C=O groups on the UHMWPE substrates, but also lead to the formation of additional amide groups. This additional amide incorporation can be explained as follows: N_2 plasma treatment can result in the cleavage of C-H bonds on the UHMWPE surface leading to the formation of polymer chain radicals at the α-amino carbons. These radicals can rapidly react with oxygen molecules in the atmosphere leading to the formation of peroxy radicals, as indicated in Fig.6. Recombination of 2 peroxy radicals can then in turn result into the formation of amides [61].

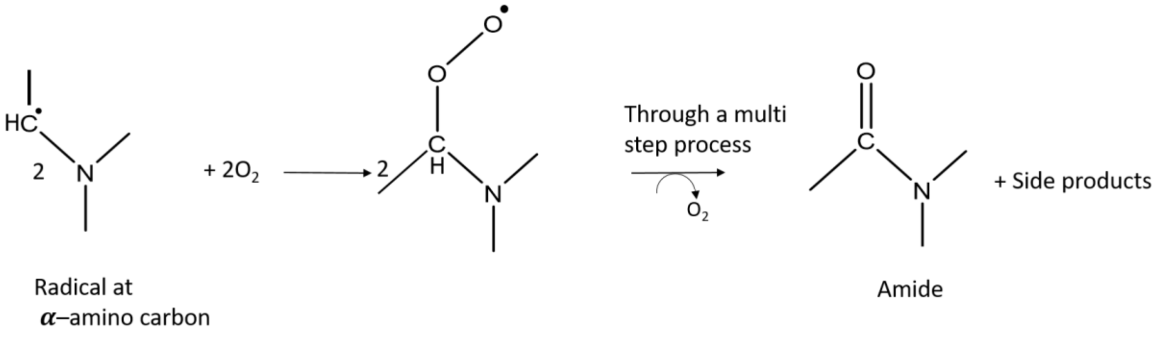

Fig.6 Mechanism responsible for the formation of amides on N_2 plasma treated UHMWPE samples upon exposure to ambient air

3.4.2 Ar plasma treatment

Table 5 shows the atomic composition of the Ar plasma modified UHMWPE samples without air exposure between plasma treatment and XPS analysis (direct sample) as well as after air exposure for time periods ranging from 5 min to 21 days. As can be seen in Table 5, as a result of the Ar plasma exposure, the oxygen concentration on the UHMWPE surface strongly increases from 1.1 ± 0.1 at% for the untreated sample to 5.9 ± 0.6 at% after Ar plasma treatment. The XPS results thus reveal that although the plasma reactor base pressure was set to 10^{-7} kPa, still a considerable amount of oxygen was incorporated on the polymer surface directly during Ar plasma exposure. Nevertheless, at higher base pressures, even higher amounts of oxygen were detected on the UHMWPE surface (Table S1). Moreover, the direct oxygen incorporation was found to be more efficient in case of the Ar plasma treatment compared to the N_2 plasma treatment, where only approximately 3 at% of oxygen was detected on the plasma treated sample. This observation is in agreement with the fact that large amounts of Ar metastables with high energy are present in the Ar discharge used in this work, as already previously mentioned [62]. These metastables can very effectively dissociate O_2 molecules in the discharge region which in turn results into higher amounts of reactive oxygen species in the plasma chamber and subsequently gives cause to a more efficient incorporation of oxygen on the polymer surface. Based on the OES spectrum of the Ar discharge (Fig.4 (b)), it can be concluded that mainly OH radicals will contribute to the oxygen incorporation processes on the UHMWPE substrates. The oxygen-rich impurities in the discharge can come from air traces remaining in the plasma reactor, from outgassing of the electrodes/dielectrics or from impurities being present in the Ar discharge gas. As already reported in literature, even small concentrations of oxygen impurities in the discharge gas (< 1 ppm) can have an large impact on the final surface chemical composition of polymers [7,21]. When examining the O/C ratio of the Ar plasma modified UHMWPE sample obtained in this work (0.06) with other O/C values mentioned in literature, it can be concluded that the oxygen incorporation is this work is considerably low. For example, in the work of Aziz et al., where a reactor base pressure of 0.05 kPa was used, a much higher O/C ratio of 0.22 was observed [53]. The considerably low oxygen incorporation in this study can be mainly attributed to the low oxygen contamination in the plasma reactor thanks to the low reactor base pressure used and the specific sample introduction procedure applied in this particular study (see Table S1). On the other hand, some studies have also reported almost no oxygen incorporation after Ar plasma treatment, however, in this case, a very special procedure was followed prior to plasma modification including baking of the plasma reactor above 100°C for 12 hours and flushing with Ar gas for 24 hours [10]. If this extended procedure was not followed, an O/C ratio of 0.04 was detected, which is slightly lower than the value observed in this work due to the fact that a lower reactor base pressure was used (10^{-9} kPa).

Table 5. Surface chemical composition of the Ar plasma modified UHMWPE samples without and with exposure to ambient air during different time periods ranging from 5 min to 21 days

Sample	**C1s (at%)**	**O1s (at%)**	**O/C**
untreated	98.9 ± 0.6	1.1 ± 0.1	0.01

direct	94.1 ± 0.6	5.9 ± 0.6	0.06
5 min	93.3 ± 0.5	6.7 ± 0.5	0.07
30 min	92.8 ± 0.7	7.2 ± 0.7	0.07
1h	92.5 ± 0.7	7.5 ± 0.7	0.08
3h	92.4 ± 0.7	7.6 ± 0.7	0.08
4h	91.4 ± 0.9	8.6 ± 0.9	0.09
6h	91.7 ± 0.4	8.3 ± 0.4	0.09
24h	88.4 ± 0.9	11.6 ± 0.9	0.13
21 days	95.7 ± 0.3	4.3 ± 0.3	0.04

Table 6. Relative concentration (in %) of carbon containing functional surface groups on UHMWPE films after Ar plasma treatment

Bands	**Untreated**	**Direct**	**5 min**	**30 min**	**1 h**	**3 h**	**4 h**	**5 h**	**6 h**	**24 h**	**21 days**
C-C	95.3 ± 0.5	87.9 ± 0.5	83.5 ± 1.7	85.5 ± 2.1	84.3 ± 1.7	80.6 ± 1.5	82.6 ± 0.2	78.6 ± 1.4	82.6 ± 1.7	78.7 ± 3.8	88.7 ± 0.3
C-O	4.6 ± 0.5	7.5 ± 0.6	10.8 ± 1.6	7.7 ± 1.3	11.1 ± 1.4	15.2 ± 0.8	11.7 ± 0.4	12.6 ± 1.0	13.6 ± 1.8	14.3 ± 2.2	7.9 ± 0.2
C=O/O-C-O	-	2.9 ± 0.2	3.3 ± 0.2	5.0 ± 2.4	3.0 ± 0.7	3.2 ± 0.5	2.9 ± 0.2	5.8 ± 0.4	3.1 ± 0.7	4.3 ± 0.6	2.2 ± 0.2
O-C=O	-	1.7 ± 0.2	2.4 ± 0.3	1.8 ± 0.7	1.6 ± 0.5	1.0 ± 0.3	2.8 ± 0.3	3.0 ± 0.5	0.7 ± 0.6	2.7 ± 2.1	1.1 ± 0.1

Table 5 also reveals that in contrast to the N_2 discharge, where nitrogen atoms are being added to the polymer surface, active Ar plasma species are not incorporated onto the polymer surface as Ar atoms are not detected on the plasma modified samples. In the case of Ar plasma treatment, the Ar plasma species most likely break C-C and/or C-H bonds present on the polymer surface, leading to the production of radical sites on the polymer backbone [20]. These radicals will subsequently react with the highly reactive oxygen species (like atomic oxygen and OH radicals) present in the Ar discharge resulting in the formation of oxygen containing functionalities on the UHMWPE surface. Table 5 also shows that after exposing the Ar plasma treated sample to ambient air for only 5 minutes, a small, but rather non-significant, increase in oxygen content can be observed. This small increase may be due to the fact that some of the carbon-centered radicals formed on the UHMWPE surface remain dangling after Ar plasma exposure: when these radicals are exposed to ambient air, they can react with oxygen molecules present in ambient air resulting in post-plasma oxidation. This result is in agreement with literature in which post-plasma oxidation processes of Ar plasma modified polyethylene samples have also been observed upon exposure to ambient air [10].

To reveal more information on the type and the relative concentration of functional oxygen groups incorporated on the UHMWPE surface upon Ar plasma treatment, high resolution C1s peaks have also been fitted according to the procedure described in the materials & methods section. In the case of Ar plasma treatment, the high resolution C1s peaks are decomposed into 4 distinct peaks as shown in Fig.2 (b): **C**-C, **C**-O, **C**=O/O-**C**-O and O-**C**=O at 285.0, 286.1, 287.3 and 289.1 eV respectively. Based on the performed C1s XPS fittings, the relative concentration of each carbon-containing surface functional group has been obtained and the results are presented in Table 6. This table reveals that Ar plasma treatment simultaneously introduces different oxygen containing groups, such as C-O, C=O/O-C-O and O-C=O bonds. Most oxygen is however incorporated in the form of C-O bonds on the Ar plasma modified UHMWPE samples, which is consistent with other XPS results available in literature [53,63]. When exposing the Ar plasma modified sample to ambient air for 5 min, a very small increase in O-C=O functionalities can be observed combined with a considerable increase in C-O functionalities, meaning that mainly C-O groups are being incorporated during post-plasma oxidation. Again, as described in the XPS section of the N_2 plasma treatment, remaining free carbon-centered surface radicals react with ambient oxygen leading to the formation of metastable peroxy radicals ($COO^{\bullet}$) as indicated in Fig.7. The reaction of $COO^{\bullet}$ with water in ambient air can then result in the formation of hydroperoxides (C-O-O-H). Additionally, combination of $COO^{\bullet}$ radicals with other $C^{\bullet}$ radicals can lead to the formation of peroxides (C-O-O-C), which can in turn decompose into $CO^{\bullet}$ radicals. Subsequent reactions between $CO^{\bullet}$ and $C^{\bullet}$ radicals can then finally result in the generation of hydroxyl or carbonyl functional groups [57]. The metastable peroxy radicals ($COO^{\bullet}$) can be also converted into $^{\bullet}COOH$ radicals via ion-radical chain reactions under particular circumstances [64]. In a subsequent step, $^{\bullet}COOH$ radicals can then react with CH resulting in the formation of O-C=O, H_2 and $C^{\bullet}$ radicals (Fig.7). In this particular case, mainly C-O and to a lesser extent O-C=O functional groups seem to appear due to the post-plasma oxidation processes, which is in contrast to the N_2 plasma treated samples on which mostly O-C=O and amide groups were post-plasma incorporated.

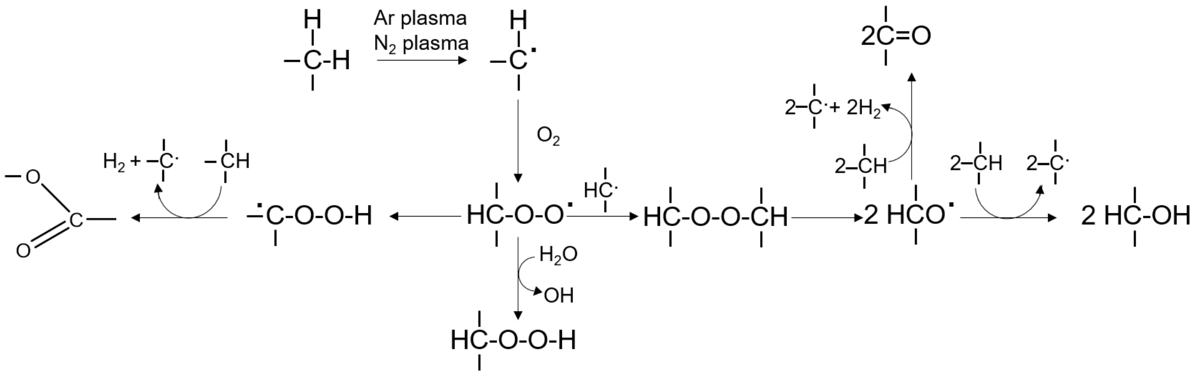

Fig.7 Possibly occurring reactions for the post-plasma oxidation of Ar and N_2 plasma treated UHMWPE samples (formation of C-O functional groups is the most pronounced in case of Ar plasma treatment; formation of O-C=O groups is the most pronounced in case of N_2 plasma treatment)

4. Ageing study of N_2 and Ar plasma treated UHMWPE samples

It is well known from literature that plasma treated polymers are susceptible to hydrophobic recovery during storage in air (the so-called ageing effect) [20,65]. The induced plasma modification is not permanent since the surface tries to reduce its surface free energy by returning as much as possible to its untreated state. In other words, the behavior of the plasma induced polar functional groups onto the surface of plasma modified polymers is known to be dynamic. The reduction in surface free energy can be possible through both reactions with ambient air as well as polymer chain reorientation/migration [17,20,65,66]. In what follows next, the objective was to find out until which time point post-plasma oxidation of the UHMWPE samples takes place and from what time point onwards the reorientation/migration of functional groups and reduction of oxygen takes the upper hand. To do so, WCA and XPS results will be discussed in the following sections and correlated with each other.

4.1. WCA results of aged N_2 and Ar plasma treated UHMWPE samples

In a first step, an ageing study of the saturated plasma treated UHMWPE surfaces was performed by repeating WCA measurements on samples stored in ambient air over a total period of 21 days and the WCA evolution as a function of storage time for N_2 and Ar plasma treated samples is presented in Fig.8 (a) and (b) respectively.

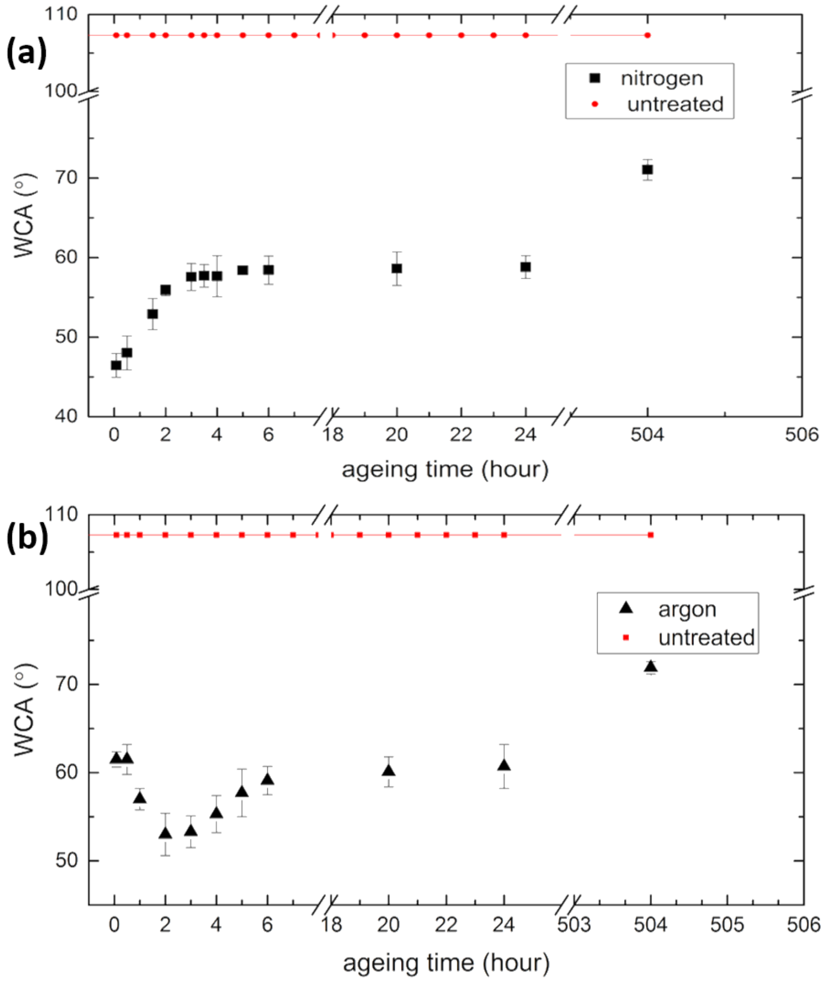

Fig.8 WCA variation as a function of ageing time for (a) N_2 and (b) Ar plasma treated UHMWPE samples

It can be observed from Fig.8 (a) that the WCA value of the N_2 plasma treated samples almost directly increases after exposing these to ambient air, similar to what has been observed by other research groups [22]. Moreover, the increase in WCA is most pronounced in the first few hours after plasma treatment, stabilizing after 5-6 hours of storage time at approximately 58.4 ± 1.8°. This WCA value is further maintained until 24 hours after plasma treatment. However, after a storage time of 21 days, it seems that the surface hydrophobic recovery does slowly progress upon longer storage, as a WCA value of 71.0 ± 1.3° is reached in this case. The observed increase in WCA values upon storage in ambient air may be attributed to the reorientation of the plasma induced polar groups into the polymer bulk or to the migration of small polymer chain fragments into the polymer matrix [20,66].

Fig.8 (b) presents the WCA evolution of Ar plasma treated samples as a function of storage time in ambient air. In this case, it can be seen that the WCA value decreases during the first 2 storage hours reaching a minimal WCA value of 53.0 ± 2.4° after 2 hours of storage in ambient air. This result is very surprising as in most cases, increases in WCA values as a function of storage time are reported for plasma modified polymers [20,65]. The decrease in WCA value during the first 2 storage hours may be due to post-plasma reactions with oxygen molecules present in ambient air resulting in the introduction of additional polar groups to the surface of the UHMWPE sample which can in turn result in the formation of a more hydrophilic surface [67]. However, after 2 hours of storage in ambient air, the WCA value starts to increase as a function of storage time until a storage time of 6 hours, after which the WCA value stabilizes at a WCA value close to the unaged Ar plasma modified sample (61.5 ± 0.8°). This stable WCA value is maintained until 24 hours after plasma treatment, after which an increase in WCA value is again noticed reaching a WCA value of 71.9 ± 0.7°after 21 days of storage. As such, after initial post-plasma reactions taken place on the Ar plasma modified samples within the first 2 hours of exposure to ambient air, the Ar plasma modified samples start to age in a similar way as the N_2 plasma treated samples.

In this results section, it is also worth mentioning that even after 21 days of ageing, the WCA values of the Ar and N_2 plasma treated samples are still considerably lower than the value of the untreated UHMWPE sample, as can be observed in Fig.8. WCA analysis thus indicates that a good UHMWPE surface wettability is preserved up until 21 days after plasma treatment, which is in close agreement with previous observations in literature [20,22,52,65,66]. Fig.8 also reveals that the ageing behavior is much more pronounced in case of the N_2 plasma treated sample as after 21 days of storage an almost similar WCA value is reached on the N_2 and Ar plasma treated samples while the N_2 plasma treated sample is much more hydrophilic prior to storage. Based on this, it could be concluded that the nitrogen containing functional groups incorporated during plasma exposure are maybe much more prone to ageing than the oxygen containing groups introduced on the polymer surface during or after plasma exposure.

4.2. XPS analysis of N_2 and Ar plasma treated UHMWPE samples during storage

4.2.1. N_2 plasma treated samples

Table 2 shows the elemental composition of the N_2 plasma treated samples as a function of storage time. As can be seen in Table 2, when storing the samples in ambient air, the nitrogen amount slightly decreases with increasing storage time from 19.8 ± 0.5 at% to 17.6 ± 1.2 at% after 24 hours of storage. This is in agreement with literature, in which a decrease in nitrogen content during ageing has also been previously observed on N_2 plasma treated polymer films [18–20,52] In this work, however, during ageing, also a small increase in oxygen amount can be seen during the first 24 hours of storage in ambient air. Table 2 also reveals that after 21 days of ageing, the surface nitrogen content strongly decreases to 8.1 ± 1.3 at% compared to the 1 day aged sample, while the oxygen content remains more or less the same.

To find possible correlations between the increase in WCA angle value observed in Fig.8 (a) and the atomic chemical composition of the UHMWPE surface during the storage of the samples in air, the O/C, (N+O)/C and N/C ratios of the N_2 plasma treated samples have also been calculated as a function of storage time and the results are given in Table 2. As expected, during the first storage day, the O/C ratio slightly increases with storage time in combination with a small decrease in N/C ratio. On the other hand, the (O+N)/C ratio remains more or less constant during the first 24 hours after plasma treatment meaning that the total amount of grafted oxygen and nitrogen atoms at the surface is not affected by 1 day of ambient exposure. As the surface wettability does decrease upon storage during the first stay, this result thus suggests that the loss in very polar nitrogen containing functional groups at the polymer surface during storage can probably not be compensated by the incorporation of additional oxygen. Table 2 also shows that after 21 days of storage, a strong decrease in N/C and (N+O)/C can be seen in combination with a slightly decreased O/C ratio compared to the 1 day aged sample. The very pronounced loss of mainly the nitrogen containing functional groups at the UHMWPE surface, which can be highly polar, can in this case explain the strongly decreased wettability when comparing the 1 day and 21 days aged samples.

In this study, the high resolution C1s and N1s peaks of the N_2 plasma treated samples have also been examined as a function of storage time and the resulting relative concentrations of the carbon and nitrogen containing functional groups can be seen in Table 3 and 4 respectively. Results reveal that during the first day of storage, the concentrations of all carbon containing bonds remain quite stable. On the other hand, when looking at the relative concentrations of the nitrogen containing bonds, some differences as a function of storage time can be seen during the first day. More specifically, the amount of primary amines decreases with increasing storage time, while the concentration of amides simultaneously increases. Other nitrogen functional groups such as C=N, secondary amides and NH_2^+ groups are almost not affected during the first storage day. This result thus suggests that during the first 24 hours of storage in air, the primary amines located at the UHMWPE surface are progressively oxidized to amides. Oxidation of primary amines to amides has already been observed by multiple other researchers when examining the ageing behavior of amino-rich plasma polymers [68,69]. Apparently, this oxidation process also occurs on N_2 plasma activated UHMWPE samples. The formation of amides at the expense of primary amines can also explain the decreased surface wettability during the first 24 hours of storage as amides are known to be less hydrophilic than primary amines [52].

When comparing the relative concentration of the carbon containing functional groups after 1 and 21 days of ageing, large differences can be seen as very strong decreases in the amount of C=O/C=N/O-C-O, O-C=N and O-C=O functional groups occur. On the other hand, the concentration of the C-O and C-N functional groups seem to remain rather unaffected. This observation can be explained as follows: during longer storage periods, the ageing behavior is no longer dominated by chemical oxidative reactions, but by the physical process of surface rearrangement in response to interfacial forces. Indeed, in contact with air, the presence of polar groups at the polymer surface is energetically unfavorable and thus polymer segments carrying such groups tend to move from the top surface into the bulk of the material [20,69,70]. As these groups migrate away from the interface, they are less detected by XPS resulting in an apparent reduction in their relative concentrations. In this particular work, mainly the polymer segments containing C=O/C=N/O-C-O, O-C=N and O-C=O bonds migrate away from the UHMWPE surface, while the C-O and C-N functional groups remain in the top surface. Most likely, these functional groups are more effectively immobilized against transport from the top surface during the N_2 plasma treatment. Moreover, the remaining of some C-O and C-N functional groups at the top surface can also explain the still enhanced surface wettability of the N_2 plasma modified sample after 21 days of storage in comparison to the untreated sample. When examining the relative concentrations of the nitrogen containing functional groups after 21 days, it can be concluded that the relative concentration of the primary amines increases, while all other nitrogen containing functional groups decrease in concentration. This result is thus in agreement with the previously shown XPS results, suggesting that all nitrogen-containing functional groups move away from the top surface, except for the remaining primary amine groups, which are more restricted from transport into the polymer bulk.

4.2.2. Ar plasma treated samples

Table 5 represents the atomic composition of the untreated and Ar plasma treated UHMWPE samples as characterized by XPS with varying ageing time. As shown there, the oxygen content and the corresponding O/C ratio considerably increases during the first 24 hours of storage suggesting that post-plasma oxidation processes not only occur within the first 5 minutes after plasma exposure (see section 3.4.2), but continue to proceed during the first day after Ar plasma exposure. Table 5 also reveals that after 21 days of storage, the total post-plasma and some of the in-plasma incorporated oxygen at the polymer surface is diffused into deeper layers as the surface oxygen content is in this case slightly lower than in case of the direct UHMWPE sample. The high resolution C1s peaks of the Ar plasma treated samples have also been examined as a function of storage time and the resulting relative concentrations of the carbon containing functional groups can be seen in Table 6. According to this table, the concentration of C-O functional groups not only increased during the first 5 minutes of air exposure, but continues to increase within the first 24 hours of storage. On the other hand, the concentration of the other oxygen containing functional groups (C=O/O-C-O and O-C=O groups) remains more or less stable during the first 24 hours of storage in ambient air.

When comparing the WCA results of the Ar plasma treated samples with their chemical composition during the first day of storage in ambient air, not a good correlation between the 2 parameters can be found. In fact, XPS measurements performed during the first 24 hours of storage show a gradual increase in surface oxygen content that should normally increase the surface wettability. However, the WCA values only decrease during the first 2 hours, after which the WCA again increases. This apparent contradiction could be explained by the different surface analyzing depth of WCA analysis and XPS: while contact angles are mostly determined by the outer few most angstroms of the polymer surface, the penetration depth of XPS is in the range of 5 to 10 nm [11,71,72]. It could therefore be possible that a high amount of C-O groups incorporated due to post-plasma oxidation processes are present at the top surface during the first 2 hours after Ar plasma treatment and that in this case only a very small amount of C-O groups is present in the subsurface layers. This situation could indeed lead to a considerably low WCA value in combination with a rather low O/C ratio. Upon further oxidation during storage, more C-O functional groups are being incorporated but it may be that more and more polymer segments containing C-O functional groups also continuously diffuse into the subsurface layers leaving only a low amount of C-O functional groups at the top surface. In this particular case, the O/C ratio of the subsurface layer can continue to increase, while the WCA value can increase.

When examining the concentrations of the carbon containing functional groups on the 1 day and 21 days aged sample, large differences in concentrations can be seen showing considerable decreases in the concentration of all plasma induced oxygen containing functionalities. This observation can be explained in a similar way as for the N_2 plasma treated samples: during longer storage periods, the ageing behavior is no longer affected by chemical oxidative reactions, but is driven by the physical process of surface rearrangement. In case of the Ar plasma treated sample, during longer storage periods, most polymer segments containing polar C-O, C=O/O-C-O and O-C=O bonds re-orientate from the

UHMWPE surface into the bulk or migrate into deeper surface layers, which can in turn explain the considerably increased WCA value of the 21 days aged sample compared to the 1 day aged sample.

5. Conclusion

The present study profoundly highlighted the relative importance of in-plasma and post-plasma surface interactions on UHMWPE samples treated with N_2 and Ar DBDs at a medium pressure of 5.0 kPa. OES results revealed the main presence of vibrational and electronically excited molecular N_2 states in the N_2 discharge, indirectly responsible for the incorporation of surface N-containing functionalities after their electron impact dissociation forming atomic nitrogen. The OES spectrum of the Ar discharge was predominantly composed of excited Ar lines but also a barely detectable line corresponding to OH radicals as trace amounts of contamination. *In-situ* XPS analysis showed a substantially high nitrogen incorporation (20.6 %) onto the polymer surface in the form of primary amines, secondary amines and amides and to a lower extend C=N and NH_2^+. This high nitrogen incorporation was accompanied by only a negligible oxygen incorporation (1.1→ 2.8 %) leading to a highly enhanced nitrogen selectivity when comparing to the current state-of-the-art. More oxygen (5.8 %) was however detected on the Ar-treated samples which is presumably due to the high energy Ar metastables capable of dissociating O_2 impurities and thus incorporating C-O, C=O and O-C=O groups. Indirect XPS analysis confirmed the occurrence of post-plasma oxidation processes illustrated by reactions between carbon-centered free radicals and ambient oxygen: O-C=O and N-C=O bonds were mainly formed on N_2-treated surfaces while C-O bonds were mostly created on Ar-treated surfaces. From a certain storage time onwards, surface polymeric chain reorientation took over the oxidation processes leading to a decreased surface wettability as a result of the migration of some pre-induced oxygen and nitrogen-containing groups away from the surface. Overall, this work sorts out basic understandings on in-plasma and post-plasma processes occurring on the surface of UHMWPE subjected to Ar and N_2 plasma activation and represents a good reference for future treatment of other polymers.

Acknowledgements

This research study was supported by a research grant (G038015N) from the Research Foundation Flanders (FWO). Parinaz Saadat Esbah Tabaei would like to thank Sara Anednatanzi and Pariviz Gohari Derakhshandeh. Rouba Ghobeira would also like to thank the FWO (grant number 12ZC720N) for financing her post-doctoral position.

References

[1] J.S. Sousa, K. Niemi, L.J. Cox, Q.T. Algwari, T. Gans, D. O’Connell, Cold atmospheric pressure plasma jets as sources of singlet delta oxygen for biomedical applications, J. Appl. Phys. 109 (2011) 123302. https://doi.org/10.1063/1.3601347.

[2] J. Lai, B. Sunderland, J. Xue, S. Yan, W. Zhao, M. Folkard, B.D. Michael, Y. Wang, Study

on hydrophilicity of polymer surfaces improved by plasma treatment, Appl. Surf. Sci. 252 (2006) 3375–3379.

[3] N. De Geyter, R. Morent, C. Leys, L. Gengembre, E. Payen, Treatment of polymer films with a dielectric barrier discharge in air, helium and argon at medium pressure, Surf. Coatings Technol. 201 (2007) 7066–7075.

[4] I. Junkar, A. Vesel, U. Cvelbar, M. Mozetič, S. Strnad, Influence of oxygen and nitrogen plasma treatment on polyethylene terephthalate (PET) polymers, Vacuum. 84 (2009) 83–85.

[5] D. Shaw, A. West, J. Bredin, E. Wagenaars, Mechanisms behind surface modification of polypropylene film using an atmospheric-pressure plasma jet, Plasma Sources Sci. Technol. 25 (2016) 065018. https://doi.org/10.1088/0963-0252/25/6/065018.

[6] T. Dufour, J. Minnebo, S. Abou Rich, E.C. Neyts, A. Bogaerts, F. Reniers, Understanding polyethylene surface functionalization by an atmospheric He/O2 plasma through combined experiments and simulations, J. Phys. D. Appl. Phys. 47 (2014). https://doi.org/10.1088/0022-3727/47/22/224007.

[7] R. Morent, N. De Geyter, L. Gengembre, C. Leys, E. Payen, S. Van Vlierberghe, E. Schacht, Surface treatment of a polypropylene film with a nitrogen DBD at medium pressure, Eur. Phys. J. Appl. Phys. 43 (2008) 289–294.

[8] B. Mészáros, G. Járvás, L. Hajba, M. Szigeti, A. Dallos, A. Guttman, Quantitative characterization of plasma treated PDMS microfluidic substrates by inverse gas chromatography, Sensors Actuators, B Chem. 258 (2018) 1184–1190. https://doi.org/10.1016/j.snb.2017.11.185.

[9] R. Ghobeira, C. Philips, L. Liefooghe, M. Verdonck, M. Asadian, P. Cools, H. Declercq, W.H. De Vos, N. De Geyter, R. Morent, Synergetic effect of electrospun PCL fiber size, orientation and plasma-modified surface chemistry on stem cell behavior, Appl. Surf. Sci. 485 (2019) 204–221. https://doi.org/10.1016/J.APSUSC.2019.04.109.

[10] S.K. Øiseth, A. Krozer, B. Kasemo, J. Lausmaa, Surface modification of spin-coated high-density polyethylene films by argon and oxygen glow discharge plasma treatments, Appl. Surf. Sci. 202 (2002) 92–103.

[11] R. Morent, N. De Geyter, C. Leys, L. Gengembre, E. Payen, Comparison between XPS- And FTIR-analysis of plasma-treated polypropylene film surfaces, in: Surf. Interface Anal., 2008. https://doi.org/10.1002/sia.2619.

[12] M. Asadian, I. Onyshchenko, D. Thiry, P. Cools, H. Declercq, R. Snyders, R. Morent, N. De Geyter, Thiolation of polycaprolactone (PCL) nanofibers by inductively coupled plasma (ICP) polymerization: Physical, chemical and biological properties, Appl. Surf. Sci. 479 (2019) 942–952. https://doi.org/10.1016/J.APSUSC.2019.02.178.

[13] M. Asadian, M. Dhaenens, I. Onyshchenko, S. De Waele, H. Declercq, P. Cools, B. Devreese, D. Deforce, R. Morent, N. De Geyter, Plasma Functionalization of Polycaprolactone Nanofibers Changes Protein Interactions with Cells, Resulting in Increased Cell Viability, ACS Appl. Mater. Interfaces. 10 (2018) 41962–41977. https://doi.org/10.1021/acsami.8b14995.

[14] R. Bitar, M. Asadian, S. Van Vrekhem, P. Cools, H. Declercq, R. Morent, N. De Geyter, Local plasma activation of PS films with a defined design for biomedical use, Surf. Coatings Technol. 350 (2018) 985–996. https://doi.org/10.1016/J.SURFCOAT.2018.03.041.

[15] F. Rezaei, M.D. Dickey, M. Bourham, P.J. Hauser, Surface modification of PET film via a large area atmospheric pressure plasma: An optical analysis of the plasma and surface characterization of the polymer film, Surf. Coatings Technol. 309 (2017) 371–381. https://doi.org/10.1016/j.surfcoat.2016.11.072.

[16] P. Nancy, J. Joy, J. James, B. Joseph, S. Thomas, N. Kalarikkal, Spectroscopic and Mass Spectrometry Analyses of Plasma-Activated Polymeric Materials, in: Non-Thermal Plasma Technol. Polym. Mater., Elsevier, 2019: pp. 319–340. https://doi.org/10.1016/b978-0-12-813152-7.00012-3.

[17] T. Desmet, T. Billiet, E. Berneel, R. Cornelissen, D. Schaubroeck, E. Schacht, P. Dubruel, Post-Plasma Grafting of AEMA as a Versatile Tool to Biofunctionalise Polyesters for Tissue Engineering, Macromol. Biosci. 10 (2010) 1484–1494.

[18] L.J. Gerenser, X-Ray photoemission study of plasma modified polyethylene surfaces, J. Adhes. Sci. Technol. 1 (1987) 303–318. https://doi.org/10.1163/156856187X00319.

[19] L.J. Gerenser, XPS studies of in situ plasma-modified polymer surfaces, J. Adhes. Sci. Technol. 7 (1993) 1019–1040.

[20] R. Morent, N. De Geyter, M. Trentesaux, L. Gengembre, P. Dubruel, C. Leys, E. Payen, Influence of Discharge Atmosphere on the Ageing Behaviour of Plasma-Treated Polylactic Acid, Plasma Chem. Plasma Process. 30 (2010) 525–536.

[21] F. Massines, G. Gouda, N. Gherardi, M. Duran, E. Croquesel, The Role of Dielectric Barrier Discharge Atmosphere and Physics on Polypropylene Surface Treatment, Plasmas Polym. 6 (2001) 35–49.

[22] G. Borcia, C.A. Anderson, N.M.D. Brown, Using a nitrogen dielectric barrier discharge for surface treatment, Plasma Sources Sci. Technol. 14 (2005) 259–267.

[23] F.M. Petrat, D. Wolany, B.C. Schwede, L. Wiedmann, A. Benninghoven, In situ ToF-SIMS/XPS investigation of nitrogen plasma-modified polystyrene surfaces, Surf. Interface Anal. 21 (1994) 274–282.

[24] M. Dhayal, M.R. Alexander, J.W. Bradley, The surface chemistry resulting from low-pressure plasma treatment of polystyrene: The effect of residual vessel bound oxygen, Appl. Surf. Sci. 252 (2006) 7957–7963. https://doi.org/10.1016/J.APSUSC.2005.10.005.

[25] B. Mutel, J. Grimblot, O. Dessaux, P. Goudmand, XPS investigations of nitrogen-plasma-treated polypropylene in a reactor coupled to the spectrometer, Surf. Interface Anal. 30 (2000) 401–406. https://doi.org/10.1002/1096-9918(200008)30:1<401::AID-SIA826>3.0.CO;2-G.

[26] L. Lianos, D. Parrat, T.Q. Hoc, T.M. Duc, Secondary ion mass spectrometry time of flight and *in situ* x-ray photoelectron spectroscopy studies of polymer surface modifications by a remote oxygen plasma treatment, J. Vac. Sci. Technol. A Vacuum, Surfaces, Film. 12 (1994) 2491–2498.

[27] A.. Meyer-Plath, K. Schröder, B. Finke, A. Ohl, Current trends in biomaterial surface functionalization—nitrogen-containing plasma assisted processes with enhanced selectivity, Vacuum. 71 (2003) 391–406.

[28] M.K. Shi, G. Dunham, M.E. Gross, G.L. Graff, P.M. Martin, Plasma treatment of PET and acrylic coating surfaces - I. In-situ XPS measurements, J. Adhes. Sci. Technol. 14 (2000) 1485–1498. https://doi.org/10.1163/156856100742320.

[29] P. Cools, S. Van Vrekhem, N. De Geyter, R. Morent, The use of DBD plasma treatment and polymerization for the enhancement of biomedical UHMWPE, Thin Solid Films. 572 (2014) 251–259.

[30] X.L. Deng, A.Y. Nikiforov, P. Vanraes, C. Leys, Direct current plasma jet at atmospheric pressure operating in nitrogen and air, J. Appl. Phys. 113 (2013) 023305.

[31] M.A. (Michael A.. Lieberman, A.J. Lichtenberg, Principles of plasma discharges and materials processing, Wiley-Interscience, 2005.

[32] J.J. Camacho, J.M.L. Poyato, L. Díaz, M. Santos, Optical emission studies of nitrogen plasma generated by IR CO2 laser pulses, J. Phys. B At. Mol. Opt. Phys. 40 (2007) 4573–4590. https://doi.org/10.1088/0953-4075/40/24/003.

[33] M.J. Fernández, O. Carabaño, M.J. van de Sande, J. Jonkers, M.C. Quintero, J.J.A.M. van der Mullen, A. Gamero, A. Sola, Preliminary spectroscopic measurements on a low-pressure argon, 2.45 GHz microwave-fed QL-lamp, J. Phys. D. Appl. Phys. 37 (2004) 1228–1233.

[34] Y. Hao, J. Chen, L. Yang, X. Wang, Lissajous figures of glow and filamentary dielectric barrier discharges under high frequency voltage at atmospheric pressure in helium, in: 2009 IEEE 9th Int. Conf. Prop. Appl. Dielectr. Mater., IEEE, 2009: pp. 626–629. https://doi.org/10.1109/ICPADM.2009.5252353.

[35] Z. Fang, T. Shao, J. Yang, C. Zhang, Discharge processes and an electrical model of atmospheric pressure plasma jets in argon, Eur. Phys. J. D. 70 (2016). https://doi.org/10.1140/epjd/e2015-60437-4.

[36] F. Bretagnol, M. Tatoulian, F. Arefi-Khonsari, G. Lorang, J. Amouroux, Surface modification of polyethylene powder by nitrogen and ammonia low pressure plasma in a fluidized bed reactor, React. Funct. Polym. 61 (2004) 221–232.

[37] A. Fridman, L.A. Kennedy, Plasma Physics and Engineering, CRC Press, 2004. https://doi.org/10.1201/9781482293630.

[38] W. Wang, B. Patil, S. Heijkers, V. Hessel, A. Bogaerts, Nitrogen Fixation by Gliding Arc Plasma: Better Insight by Chemical Kinetics Modelling, ChemSusChem. 10 (2017) 2145–2157. https://doi.org/10.1002/cssc.201700095.

[39] R. Snoeckx, S. Heijkers, K. Van Wesenbeeck, S. Lenaerts, A. Bogaerts, CO $_2$ conversion in a dielectric barrier discharge plasma: N $_2$ in the mix as a helping hand or problematic impurity?, Energy Environ. Sci. 9 (2016) 999–1011. https://doi.org/10.1039/C5EE03304G.

[40] A.J. Wagner, D.H. Fairbrother, F. Reniers, A Comparison of PE Surfaces Modified by

Plasma Generated Neutral Nitrogen Species and Nitrogen Ions, Plasmas Polym. 8 (2003) 119–134. https://doi.org/10.1023/A:1023942211714.

[41] S.B. Bayram, M. V Freamat, Vibrational spectra of N 2 : An advanced undergraduate laboratory in atomic and molecular spectroscopy, (2012). https://doi.org/10.1119/1.4722793.

[42] N. Sewraj, N. Merbahi, J.P. Gardou, P.R. Akerreta, F. Marchal, Electric and spectroscopic analysis of a pure nitrogen mono-filamentary dielectric barrier discharge (MF-DBD) at 760 Torr, J. Phys. D. Appl. Phys. 44 (2011). https://doi.org/10.1088/0022-3727/44/14/145201.

[43] Alexander Fridman, Plasma Chemistry , 2008.

[44] M. Capitelli, C. Ferreira, B. Gordiets, A. Osipov, Plasma kinetics in atmospheric gases, 2013.

[45] NIST Atomic Spectra Database, (2019). https://doi.org/https://doi.org/10.18434/T4W30F.

[46] R. Brandenburg, J. Ehlbeck, M. Stieber, T. v. Woedtke, J. Zeymer, O. Schlüter, K.-D. Weltmann, Antimicrobial Treatment of Heat Sensitive Materials by Means of Atmospheric Pressure Rf-Driven Plasma Jet, Contrib. to Plasma Phys. 47 (2007) 72–79. https://doi.org/10.1002/ctpp.200710011.

[47] X. Fei, S.I. Kuroda, Y. Kondo, T. Mori, K. Hosoi, Influence of additive gas on electrical and optical characteristics of non-equilibrium atmospheric pressure argon plasma jet, Plasma Sci. Technol. 13 (2011) 575–582. https://doi.org/10.1088/1009-0630/13/5/13.

[48] G. Aziz, N. De Geyter, H. Declercq, R. Cornelissen, R. Morent, Incorporation of amine moieties onto ultra-high molecular weight polyethylene (UHMWPE) surface via plasma and UV polymerization of allylamine, Surf. Coatings Technol. 271 (2015) 39–47. https://doi.org/10.1016/J.SURFCOAT.2015.01.027.

[49] S. Van Vrekhem, P. Cools, H. Declercq, A. Van Tongel, C. Vercruysse, M. Cornelissen, N. De Geyter, R. Morent, Application of atmospheric pressure plasma on polyethylene for increased prosthesis adhesion, Thin Solid Films. 596 (2015) 256–263. https://doi.org/10.1016/J.TSF.2015.08.055.

[50] N. De Geyter, R. Morent, T. Desmet, M. Trentesaux, L. Gengembre, P. Dubruel, C. Leys, E. Payen, Plasma modification of polylactic acid in a medium pressure DBD, Surf. Coatings Technol. 204 (2010) 3272–3279. https://doi.org/10.1016/j.surfcoat.2010.03.037.

[51] P. Cools, M. Asadian, W. Nicolaus, H. Declercq, R. Morent, N. De Geyter, Surface Treatment of PEOT/PBT (55/45) with a Dielectric Barrier Discharge in Air, Helium, Argon and Nitrogen at Medium Pressure, Materials (Basel). 11 (2018) 391. https://doi.org/10.3390/ma11030391.

[52] A. Vesel, I. Junkar, U. Cvelbar, J. Kovac, M. Mozetic, Surface modification of polyester by oxygen- and nitrogen-plasma treatment, Surf. Interface Anal. 40 (2008) 1444–1453.

[53] G. Aziz, P. Cools, N. De Geyter, H. Declercq, R. Cornelissen, R. Morent, Dielectric

barrier discharge plasma treatment of ultrahigh molecular weight polyethylene in different discharge atmospheres at medium pressure: A cell-biomaterial interface study, Biointerphases. 10 (2015) 029502. https://doi.org/10.1116/1.4907755.

[54] R. Dorai, M.J. Kushner, A model for plasma modification of polypropylene using atmospheric pressure discharges, J. Phys. D. Appl. Phys. 36 (2003) 666–685. https://doi.org/10.1088/0022-3727/36/6/309.

[55] N. Vandencasteele, F. Reniers, Plasma-modified polymer surfaces: Characterization using XPS, J. Electron Spectros. Relat. Phenomena. 178–179 (2010) 394–408. https://doi.org/10.1016/J.ELSPEC.2009.12.003.

[56] G. Borcia, C.A. Anderson, N.M.D. Brown, Dielectric barrier discharge for surface treatment: application to selected polymers in film and fibre form, Plasma Sources Sci. Technol. 12 (2003) 335–344. https://doi.org/10.1088/0963-0252/12/3/306.

[57] T.R. Gengenbach, Z.R. Vasic, R.C. Chatelier, H.J. Griesser, A multi-technique study of the spontaneous oxidation of N-hexane plasma polymers, J. Polym. Sci. Part A Polym. Chem. 32 (1994) 1399–1414. https://doi.org/10.1002/pola.1994.080320801.

[58] A. Manakhov, P. Skladal, M. Elias, J. Cechal, J. Polak, D. Necas, L. Zajickova, Pulsed Plasma Polymerization of Cyclopropylamine for Deposition of Stable Amine-Rich Films Aimed at the Bio-Immobilization Applications, in: Soc. Vac. Coaters 57th Annu. Tech. Conf. Proc., Society of Vacuum Coaters, 2015: pp. 504–512. https://doi.org/10.14332/svc14.proc.1877.

[59] A. Manakhov, E. Makhneva, P. Skládal, D. Nečas, J. Čechal, L. Kalina, M. Eliáš, L. Zajíčková, The robust bio-immobilization based on pulsed plasma polymerization of cyclopropylamine and glutaraldehyde coupling chemistry, Appl. Surf. Sci. 360 (2016) 28–36. https://doi.org/10.1016/j.apsusc.2015.10.178.

[60] A. Manakhov, L. Zajíčková, M. Eliáš, J. Čechal, J. Polčák, J. Hnilica, Š. Bittnerová, D. Nečas, Optimization of cyclopropylamine plasma polymerization toward enhanced layer stability in contact with water, Plasma Process. Polym. 11 (2014) 532–544. https://doi.org/10.1002/ppap.201300177.

[61] T.R. Gengenbach, H.J. Griesser, Aging of 1,3-diaminopropane plasma-deposited polymer films: Mechanisms and reaction pathways, J. Polym. Sci. Part A Polym. Chem. 37 (1999) 2191–2206.

[62] R.J. Leiweke, B.N. Ganguly, Effects of pulsed-excitation applied voltage rise time on argon metastable production efficiency in a high pressure dielectric barrier discharge, Appl. Phys. Lett. 90 (2007). https://doi.org/10.1063/1.2748324.

[63] A. Van Deynse, N. De Geyter, C. Leys, R. Morent, Influence of water vapor addition on the surface modification of polyethylene in an argon dielectric barrier discharge, Plasma Process. Polym. 11 (2014) 117–125. https://doi.org/10.1002/ppap.201300088.

[64] M. Lazár, J. Rychlý, Oxidation of hydrocarbon polymers, Adv. Polym. Sci. 102 (1992) 189–221. https://doi.org/10.1007/3-540-55090-9_7.

[65] R. Morent, N. De Geyter, C. Leys, L. Gengembre, E. Payen, Study of the ageing behaviour of polymer films treated with a dielectric barrier discharge in air, helium

and argon at medium pressure, Surf. Coatings Technol. 201 (2007) 7847–7854.

[66] A. Van Deynse, P. Cools, C. Leys, R. Morent, N. De Geyter, Influence of ambient conditions on the aging behavior of plasma-treated polyethylene surfaces, Surf. Coatings Technol. 258 (2014) 359–367. https://doi.org/10.1016/J.SURFCOAT.2014.08.073.

[67] F. Rezaei, B. Shokri, M. Sharifian, Atmospheric-pressure DBD plasma-assisted surface modification of polymethyl methacrylate: A study on cell growth/proliferation and antibacterial properties, Appl. Surf. Sci. 360 (2016) 641–651.

[68] G. Aziz, M. Thukkaram, N. De Geyter, R. Morent, Plasma parameters effects on the properties, aging and stability behaviors of allylamine plasma coated ultra-high molecular weight polyethylene (UHMWPE) films, Appl. Surf. Sci. 409 (2017) 381–395. https://doi.org/10.1016/j.apsusc.2017.03.027.

[69] T.R. Gengenbach, R.C. Chatelier, H.J. Griesser, Correlation of the nitrogen 1s and oxygen 1s XPS binding energies with compositional changes during oxidation of ethylene diamine plasma polymers, Surf. Interface Anal. 24 (1996) 611–619. https://doi.org/10.1002/(SICI)1096-9918(19960916)24:9<611::AID-SIA169>3.0.CO;2-7.

[70] T.F. Chen, K.S. Siow, P.Y. Ng, B.Y. Majlis, Enhancing the biocompatibility of the polyurethane methacrylate and off-stoichiometry thiol-ene polymers by argon and nitrogen plasma treatment, Mater. Sci. Eng. C. 79 (2017) 613–621. https://doi.org/10.1016/j.msec.2017.05.091.

[71] R. Morent, N. De Geyter, F. Axisa, N. De Smet, L. Gengembre, E. De Leersnyder, C. Leys, J. Vanfleteren, M. Rymarczyk-Machal, E. Schacht, E. Payen, Adhesion enhancement by a dielectric barrier discharge of PDMS used for flexible and stretchable electronics, J. Phys. D. Appl. Phys. 40 (2007) 7392–7401. https://doi.org/10.1088/0022-3727/40/23/021.

[72] S. Van Vrekhem, K. Vloebergh, M. Asadian, C. Vercruysse, H. Declercq, A. Van Tongel, L. De Wilde, N. De Geyter, R. Morent, Improving the surface properties of an UHMWPE shoulder implant with an atmospheric pressure plasma jet, Sci. Rep. 8 (2018) 4720. https://doi.org/10.1038/s41598-018-22921-6.